JOURNAL OF MATERIALS SCIENCE 18 (1983) 1583–1589

Pentavalent vanadium ion addition to Ni–Zn ferrites

Part 1 *Microstructure and grain-growth kinetics*

R. NARAYAN, R. B. TRIPATHI, B. K. DAS, G. C. JAIN
Division of Materials, National Physical Laboratory, Hillside Road, New Delhi-110012, India

Systematic studies of the changes in microstructure and the grain-growth kinetics of iron-deficient and iron-excess Ni–Zn ferrites with varying contents of V_2O_5 have been undertaken. The basic composition of an iron-deficient Ni–Zn ferrite showed a duplex structure. Modified microstructures with pore-free and uniform grains were obtained on V_2O_5 doping. A regular increase in grain size was found with increasing V_2O_5 content both in iron-deficient and iron-excess compositions. The square of the average grain diameter varied linearly with sintering time up to 0.0 to 0.4 mol % V_2O_5. For higher V_2O_5 contents (0.6 to 1.0 mol %), the cube of the average grain diameter was directly proportional to the sintering time. Modifications in the microstructure and the grain growth have been explained in terms of the solubility of V_2O_5 in the lattice and liquid-phase formation at the grain boundaries.

1. Introduction

The influence of grain size, porosity and orientation of crystallites on the magnetic properties of practical importance is considerable. Densification and grain growth all occur simultaneously during sintering and give rise to a great variety of microstructures; subtle changes in the impurity contents, the packing of powders and processing parameters also affect the microstructure. The use of a second phase to control grain growth is well known from the literature [1–4]. An additive forming a liquid phase during sintering gives rise to pore-free grains and faster densification in a short time [5]. Impurities going into solid solution change the defect structure of the host material and affect the microstructure and densification accordingly. Jain *et al.* [6] have shown that small amounts of V_2O_5 affect the densification of Ni–Zn ferrites drastically. Various workers [7–9] have studied the effect of various additives on grain-growth kinetics and the microstructure of Mn–Zn ferrites. However, no systematic work has been undertaken to study the kinetics of grain growth and changes in the microstructure as a function of various additives in Ni–Zn ferrites.

This paper presents a systematic study of the kinetics of grain growth and the changes in microstructure of iron-deficient and iron-excess Ni–Zn ferrites as a function of V_2O_5 content of the ferrites.

2. Experimental procedure

Sets of iron-excess (IE) and iron-deficient (ID) Ni–Zn ferrites were prepared by the method described elsewhere [6]:

(1) $Ni_{0.58}Zn_{0.40}Fe_{2.02}O_4 + x\,V_2O_5$ iron-excess composition;

(2) $Ni_{0.62}Zn_{0.40}Fe_{1.98}O_4 + x\,V_2O_5$ iron-deficient composition; where the values of x were 0.002, 0.004, 0.006, 0.008 and 0.01.

A thin layer (1 mm) was lapped off both the sides of each of the sintered tablets. After ultrasonic cleaning in trichloroethylene, the samples were polished with diamond paste of different grades. The polished specimens were etched thermally at a temperature of about 100 to 200° C below their normal sintering temperatures for 1

0022–2461/83 $03.00 + .12

to 5 min to reveal their microstructure. Some of the samples which were oxidized during thermal etching were chemically etched. The chemical etching was performed in a 1:1 (by volume) mixture of sulphuric acid and saturated solution of oxalic acid at the boiling temperature of the mixture.

Measurement of the average grain size of the samples was done by counting the number of grain boundaries intersected by a measured length of random straight line drawn on the photograph of the etched sections [10]. The average grain size, $\bar{D}$, was computed from the relation $\bar{D} = K\bar{L}$, where $\bar{L}$, is the average concept size of the grain and K is a proportionality constant. For spherical grain geometry with uniform size distribution, which is reasonably true in our case, K assumes a value of 1.5 [11].

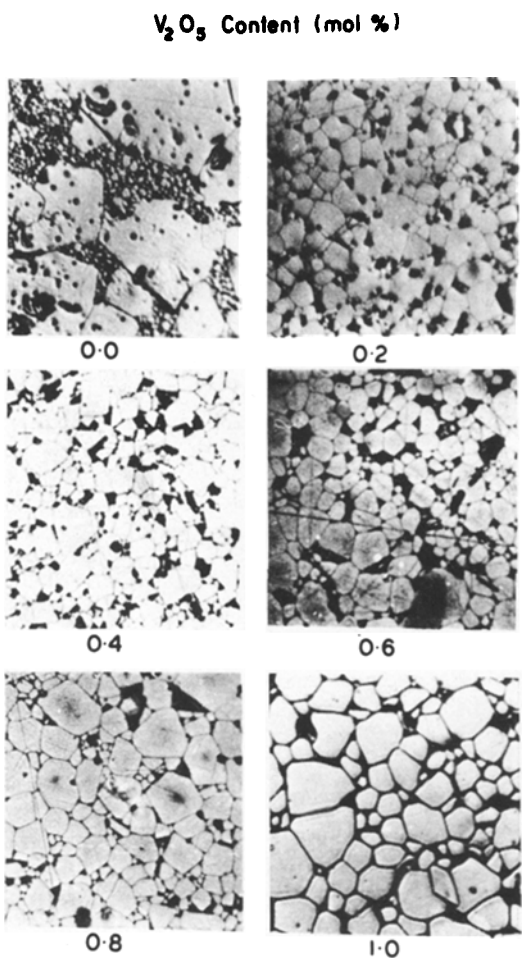

Figure 1 Microstructures of iron-deficient Ni–Zn ferrite compositions containing 0.0 to 1.0 mol% V_2O_5 sintered at 1200° C for 2 h, × 900.

3. Experimental results

Metallographic examination of the polished and etched surfaces of the samples of different batches revealed several microstructural features described in the following sections.

3.1. Iron-deficient (ID) compositions

The microstructure of the iron-deficient ferrites containing various amounts of V_2O_5 sintered at different temperatures (1100 to 1300° C) in air for different times (0.5 to 8 h) were observed. As an example, Fig. 1 depicts the microstructure of ID Ni–Zn ferrites containing 0 to 0.1 mol% V_2O_5 sintered at 1200° C for 2 h in air. The basic composition exhibited the duplex granular structure, i.e. small pores per grain present along with a few giant grains having many isolated pores trapped inside the grains. The sample containing 0.2 mol% V_2O_5 showed pore-free grains of uniform size, having an average grain size greater than the average size of the pore-free grains of the basic ID compositions. With further addition of V_2O_5, the average grain size increased without any substantial change in the granular structure. Figs. 2 and 3 show plots of average grain size determined from micrographs of samples against the sintering time at various sintering

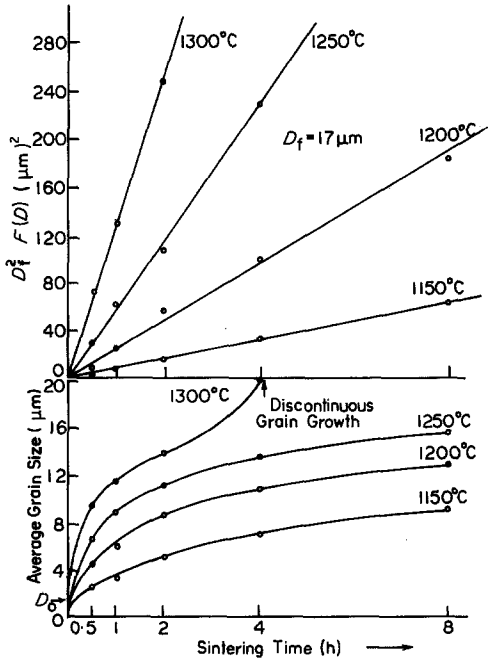

Figure 2 Grain-growth isotherm (lower part) and plots of Burke's equation, $D^2 - D_0^2 = Kt$ (lower part) for an iron-deficient composition containing 0.4 mol% V_2O_5.

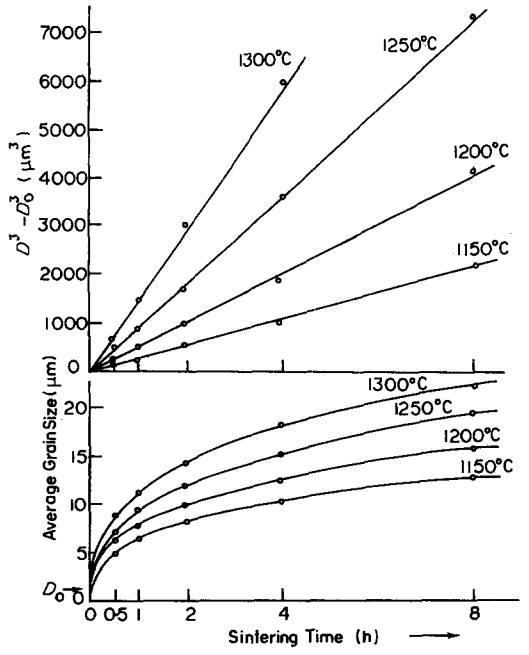

Figure 3 Grain-growth isotherms (lower part) and plots of $D^3 - D_0^3 = Kt$ (upper part) for an iron-deficient composition containing 1.0 mol% V_2O_5.

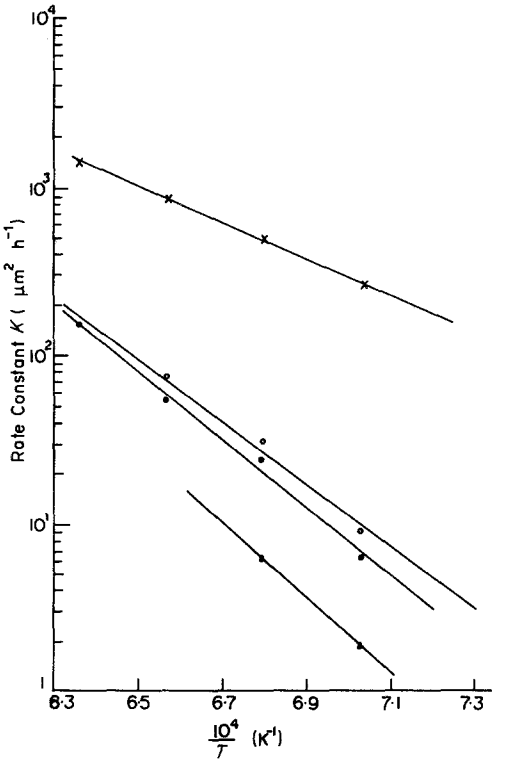

Figure 4 Arrhenius plots of the rate constant, K, against $1/T$ for iron-deficient compositions containing V_2O_5: ▲, 0.0 mol%; ●, 0.2 mol%; ○, 0.4 mol%; and ×, 1.0 mol%.

temperatures for ID compositions containing 0.4 and 1.0 mol% V_2O_5. The upper part of Fig. 2 shows that the square of the average grain diameter, $\bar{D}$, has a linear relation to the sintering time, t, and fits very well to the Burke's equation [12], i.e.

$$D_f^2\left[\frac{D-D_0}{D_f}+\ln\frac{D_f-D_0}{D-D_0}\right] = Kt \qquad (1)$$

where D_f is limiting grain size, D_0 is the grain size at $t = 0$ and K is the rate constant. In Fig. 3, the upper part depicts the plot of $(D^3 - D_0^3)$ against sintering time at different sintering temperatures. The data shown in Fig. 3 fit very well the Lay [13] equations, i.e.

$$D^3 - D_0^3 = Kt. \qquad (2)$$

In the upper part of all the figures, the solid lines are the lines of regression and their slopes give the value of the rate constant K. The rate constant, K, in Equation 2 is expressed by the Arrhenius equation

$$K = K_0 \exp(-E/RT) \qquad (3)$$

where K_0 is a constant, E is the activation energy of the grain growth, R is the gas constant and T is the absolute temperature. The activation energies are computed from the slopes of $\log K$ against $1/T$ curves shown in Fig. 4 for 0.0, 0.2, 0.4 and 1.0 mol% V_2O_5 listed in Table I.

3.2. Iron-excess (IE) compositions

Fig. 5 exhibits the microstructure of iron-excess ferrites with different V_2O_5 contents sintered at 1200° C for 2 h in air. It was found that the grain size increased monotonically with increasing addition of V_2O_5. All the samples except one containing 0.2 mol% V_2O_5 exhibited pore-free grains. The microstructure of the sample con-

TABLE I Activation energy of grain growth of iron-deficient and iron-excess Ni–Zn ferrites for various V_2O_5 contents

V_2O_5 content (mol%)	Activation energy of grain growth (kcal mol^{-1})	
	Iron deficient	Iron excess
0.0	101	95
0.2	92	82
0.4	84	81
0.6	46	49
0.8	60	50
1.0	49	46

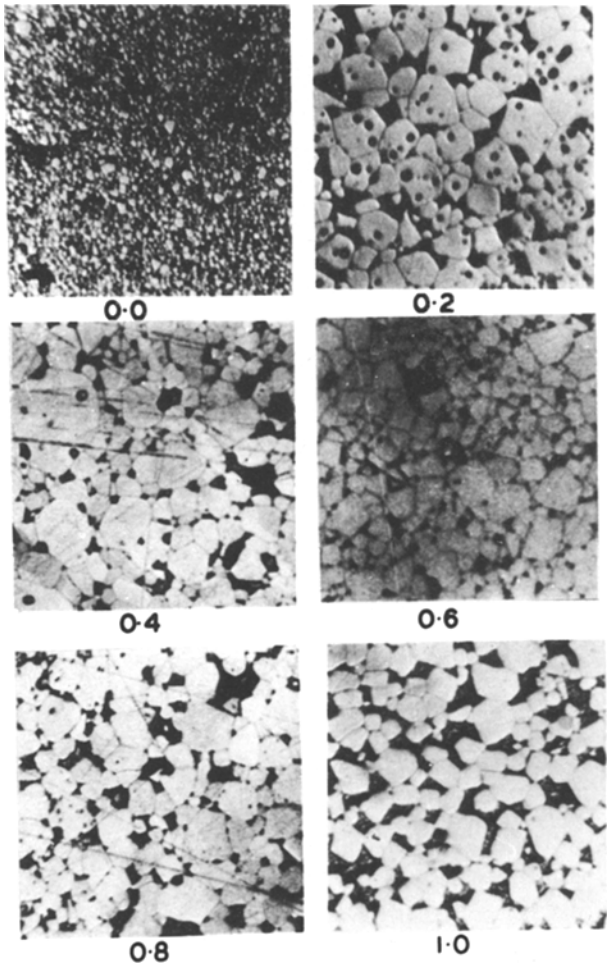

Figure 5 Microstructures of iron-excess Ni–Zn ferrite compositions containing 0.0 to 1.0 mol % V_2O_5 sintered at 1200° C for 2 h, × 900.

taining 0.2 mol % V_2O_5 showed some intragranular porosity although the grain growth was normal. Figs. 6 and 7 show the plots of average grain size determined from the micrographs of samples sintered at different temperatures (1100 to 1300° C) for different times (0.5 to 8 h) against the sintering times at various temperatures. The upper part of Fig. 6 shows a plot of $D^2 F(D)$ against t, whereas that of Fig. 7 shows $D^3 - D_0^3$ against time. In the upper parts of these figures the continuous lines are regression lines, whereas the circles are the experimental points. The slopes of these lines give the value of the rate constant, K. The active slope of the $\log K$ against $1/T$ curves (Fig. 8) and are tabulated in Table I.

4. Discussion

Jain *et al.* [6] have shown that V_2O_5 is partially soluble in both the iron-excess and iron-deficient ferrites. The maximum density was observed at a V_2O_5 content of 0.4 mol %. If vanadium enters a solid solution with ferrites as V^{5+} ions, then for every addition of V^{5+} ions, 7/3 Fe^{3+} ions will be reduced to 7/3 Fe^{2+} ions to satisfy charge and site balance, increasing the Fe^{2+}/Fe^{3+} ratio. The oxidation reduction equation of iron in ferrite gives

$$Fe^{2+} + \tfrac{1}{4}O_2(g) \rightleftharpoons Fe^{3+} + \tfrac{3}{8}V_{Fe} + \tfrac{1}{2}O_0^{2-}$$

or

$$[V_{Fe}]^{3/8} \rightarrow K_{23} \frac{[Fe^{2+}]P_{O_2}^{1/4}}{[Fe^{3+}][O_0^{2-}]^{1/2}} \qquad (4)$$

where V_{Fe} denotes iron vacancy concentration and K_{23} is the redox equilibrium constant. At the same temperature an increase in the Fe^{2+}/Fe^{3+} ratio, would cause an increase in the cation (or Fe) vacancy concentration and hence a decrease in

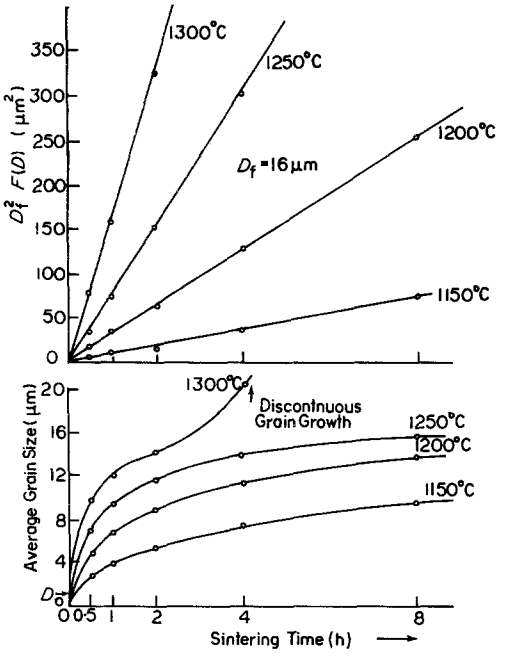

Figure 6 Grain-growth isotherms (lower part) and plots of Burke's equation $D^2 - D_0^2 = Kt$ (upper part) for iron-excess compositions containing 0.4 mol% V_2O_5.

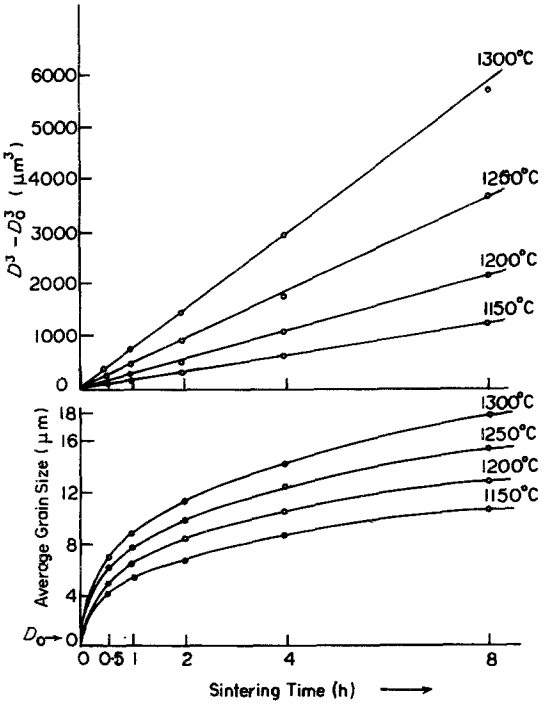

Figure 7 Grain-growth isotherms (lower part) and plots of $D^3 - D_0^3 = Kt$ (upper part) for ion-excess compositions containing 1.0 mol% V_2O_5.

anion (oxygen) vacancy concentration. Dissolution of V_2O_5 in ferrites will, therefore, lead to a decrease in oxygen vacancy concentration and hence oxygen ion diffusivity. An overall examination of the microstructure of ID and IE compositions reveals the following features:

(1) samples containing 0.0 to 0.4 mol% V_2O_5 exhibited discontinuous grain growth after a certain sintering product whereas the sample containing a higher amount of V_2O_5 (1 mol%) did not show discontinuous grain growth in the sintering time and temperature range studied.

(2) the average grain size/time data of a sample containing V_2O_5 up to 0.4 mol% were found to obey the Burke [12] equation of grain-growth kinetics whereas those containing higher amounts of V_2O_5 ($\geqslant$ 0.6 mol%) obeyed Equation 2;

(3) the limiting grain size was found to increase with the addition of V_2O_5.

There is an excess anion vacancy concentration in the basic iron-deficient ferrite; therefore, secondary or discontinuous grain growth starts in these samples at comparatively lower sintering temperatures and/or shorter sintering times. As could be seen from Fig. 1, when 0.2 mol% V_2O_5 is added to these samples, the secondary grain growth is suppressed owing to a decrease in anion vacancy concentration as per Equation 4 which, in turn, decreases the grain mobility. In the ID samples containing 0.4 mol% V_2O_5, the grain-boundary mobility is further reduced leading to a further suppression of discontinuous grain growth. The microstructure of samples containing higher amounts of V_2O_5 (0.6 to 1.0 mol%) exhibit large grains having big pores at the grain boundaries. This can be attributed to the liquid phase present during the sintering of these samples. As reported by Lay [13] and argued by Burke [12], the presence of a liquid phase during sintering accelerates the rate of grain growth and the coalescence of fine pores in to the larger ones. The rounding of the grains and the sharp decrease in the activation energy of grain growth and of densification observed in the sample containing $\geqslant$ 0.6 mol% V_2O_5 suggests that at the sintering temperature the grains are separated by a liquid phase. The presence of a liquid phase for a sample containing 1.0 mol% V_2O_5 has also been confirmed by metallographic examination.

The basic iron-excess composition exhibits a microstructure of uniformly distributed small pore-free grains. This is because of the low mobility of the grain boundary in this composition. The microstructure of IE composition containing

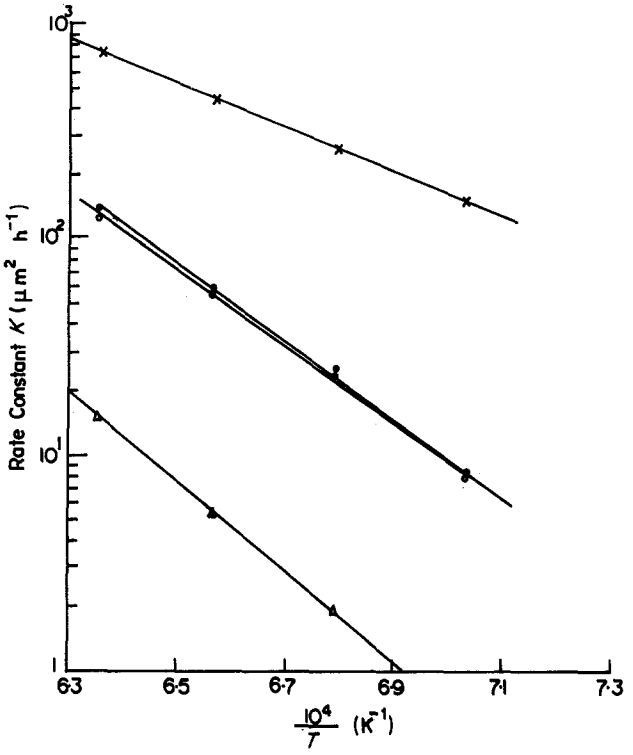

Figure 8 Arrhenius plots of the rate constant K against $1/T$ for iron-excess compositions containing V_2O_5: ▲, 0.0 mol%; ●, 0.2 mol%; ○, 0.4 mol%, and ×, 1.0 mol%.

0.2 mol% V_2O_5 exhibits a larger average grain size compared to the basic IE composition. This enlargement of grain size can be described as follows. As the ferrite was calcined at 900° C for 2 h, there would be some unreacted V_2O_5 present in the calcined powder. On initial heating during sintering, this unreacted V_2O_5 would form a V_2O_5-rich liquid phase leading to an increased rate of densification and large grain size. However, when calcination was carried out at 1100° C for 2 h, the density and grain size of ferrite containing 0.2 mol% V_2O_5 was less than the basic composition. This is due to the unreacted V_2O_5 dissolving into the ferrite matrix completely during calcining and hence resulting in a decreased oxygen vacancy concentration, thereby slowing the sintering and grain-growth rates. The microstructures of samples containing 0.4 mol% V_2O_5 shows pore-free grains having comparatively larger pores at grain boundaries. In this composition, the pore mobility has increased as in the Reijnen model [14, 15]. This explains the pore-free grains and large pores at grain boundaries as observed in these samples.

The large grains and pores at grain boundaries observed in the sample containing $V_2O_5 \geqslant 0.6$ mol % can be attributed to the liquid-phase sintering as explained in the case of ID compositions.

4.1. Grain growth kinetics

The data of the present studies have been found to fit the Burke equation for 0 to 0.4 mol% V_2O_5 content. It has been found that D_f increases with an increase in V_2O_5 content in both IE and ID composition. The increase in the limiting grain size with the addition of V_2O_5 is due to two factors:

(1) increase in cation vacancy concentration resulting in higher pore mobility;

(2) owing to the presence of a liquid phase during the initial part of sintering, pore coalescence, resulting in large pores, occurs before grain growth controlled by bulk diffusion starts.

For higher contents of V_2O_5 (0.6 to 1.0 mol%) the data were found to fit Equation 2 well. This is in good agreement with the Lay equation for grain-growth kinetics for sintering in the presence of a liquid phase and the grain-growth kinetics observed by Nicholson [16] in the study of the sintering of MgO in the presence of a liquid phase.

4.2. Activation energy

Within experimental error, the activation energy has been found to be the same for all ID and IE compositions containing V_2O_5 up to 0.4 mol% in the present studies. This value is in good agreement with that found by Paulus [2, 3], Iimura

[17] and Jain *et al.* [18] in the case of Mn–Zn ferrites. Therefore, this indicates that in these samples, the grain growth is controlled by the solid-state diffusion of oxygen ions at the later stage of sintering.

ID and IE compositions having $V_2O_5 \geqslant 0.6$ mol % show a sharp decrease in activation energy. This can be attributed to the presence of liquid-phase during the sintering. The decrease in activation energy of grain growth in the presence of a liquid phase as observed in the present studies is also consistent with the findings of Jain *et al.* [18] and Nicholson [16].

Acknowledgement

The authors wish to express their appreciation to Dr A. R. Verma, Director, National Physical Laboratory, for granting permission to publish this work.

References

1. P. D. BABA, *J. Amer. Ceram. Soc.* **48** (1965) 305.
2. M. PAULUS and CH. GUILAUD, *J. Phys. Soc. Japan* **17** (1967) 632 Suppl. B-1.
3. M. PAULUS, *Phys. Stat. Sol.* **2** (1962) 118, 1325.
4. *Idem, Mat. Sci. Res.* **3** (1966) 31.
5. W. D. KINGERY (ed), "Ceramic Fabrication processes" (M.I.T. Press, Cambridge, 1963).
6. G. C. JAIN, B. K. DAS, R. B. TRIPATHI and R. NARAYAN, *J. Mag. Mag. Mater.* **14** (1979) 80.
7. A. L. STUIJTS, *Proc. Brit. Ceram. Soc.* **2** (1964) 73.
8. A. D. GILES and F. F. WESTENDROP, *J. De Physique I.C.F.* **2**, Colloque C1 suppl. an No. 4 Tome **38** (1977) P C1-317.
9. G. ROSSI and J. E. BURKE, *J. Amer. Ceram. Soc.* **56** (1973) 654.
10. N. C. GOEL, Ph.D. Thesis, University of Delhi (1977).
11. R. L. FULLMAN, *Trans AIME* **197** (1953) 447, 1267.
12. J. E. BURKE, *ibid.* **180** (1949) 73.
13. K. W. LAY, *J. Amer. Ceram. Soc.* **51** (1968) 373.
14. P. J. L. REIJNEN, Science of Ceramics, Vol. 4, edited by G. H. Stewart (The British Ceramic Society, 1968) p. 169.
15. A. RABENAU (ed), "Problems of Non-Stoichiometry" (North-Holland, Amsterdam, 1970) p. 219.
16. G. C. NICHOLSON, *J. Amer. Ceram. Soc.* **48** (1965) 525.
17. T. IIMURA, *Proc. Int. Conf. Ferrites, Japan* **1** (1970) 128.
18. G. C. JAIN, B. K. DAS and N. C. GOEL, *Ind. J. Pure Appl. Phys.* **14** (1976) 87.

Received 23 April
and accepted 15 July 1982